# Glucose-sulfate conjugates as a new phase-2 metabolite formed by aquatic crustaceans

Yoshinori Ikenaka[1], Masumi Ishizaka[2], Heesoo Eun[2], Yuichi Miyabara[1]

[1] Division of Science for Inland Water Environment, Institute of Mountain Science, Shinshu University, 5-2-4 Kogandori Suwa, Nagano 392-0027, Japan
[2] National Institute for Agro-Environmental Sciences, 3-1-3, Kannondai, Tsukuba, Ibaraki 305-8604, Japan

Corresponding author
Name: Yoshinori Ikenaka
Address: Division of Science for Inland Water Environment, Institute of Mountain Science, Shinshu University, 5-2-4 Kogandori Suwa, Nagano 392-0027, Japan
TEL: +81-266-52-1955
FAX: +81-266-57-1341
E-mail address: y_ikenaka@hotmail.com

## Abstract
We found that aquatic crustaceans, decapoda; atyidae (*Caridina multidentata*, *Neocaridina denticulate*, and *Paratya compressa*), metabolize pyrene to a new conjugation product. The results of deconjugation treatments indicated that glucose and sulfate combined with 1-hydroxypyrene. Further analysis by LC/ESI-MS/MS showed that the molecular weight of the product was 460 (*m/z* 459; deprotonated ion), and that it has a glucose-sulfate moiety (*m/z* 241; fragment ion). These results indicated that the new metabolite was the glucose-sulfate conjugate of 1-hydroxypyrene. The glucose-sulfate conjugate is a phase-2 product that has not been reported previously from any organism. Several studies have demonstrated that sulfation is an important pathway for metabolism of xenobiotics in aquatic invertebrates. Thus, glucose-sulfate conjugates may add an important signal for excretion or sequestration of xenobiotics for aquatic invertebrates.

## Keywords
Crustacean; Shrimp; Xenobiotics; Polycyclic aromatic hydrocarbons; Pyrene; Metabolism; Cytochrome P450; Phase-2; Conjugation; Glucose-sulfate conjugation

# 1. Introduction

Organisms show a wide degree of variation in the ability to metabolize xenobiotics [1]. These variations cause a range of tolerance between species. Metabolism of xenobiotics is carried out mainly in the liver and in the mid-gut gland, the hepatopancreas, in vertebrates and invertebrates, respectively. Metabolism is often classified into three phases: phase-1 (oxidation), phase-2 (conjugation), and phase-3 (excretion). Phase-1 is mediated primarily by the cytochrome P450 (CYP) family of microsomal enzymes [2, 3]. The phase-1 oxidative reaction adds specific sites where the phase-2 process can then occur [2]. Phase-2 reactions are condensations of xenobiotics or phase-1 products with biomolecules. This process can increase the molecular weight and generally increase the water-solubility of xenobiotics [2]. Phase-3 processes result in excretion of metabolites by membrane proteins, such as ATP binding cassette (ABC) transporters [4 – 6], as phase-2 conjugates are typically too hydrophilic to passively diffuse across the cell membrane [2].

Several previous studies have indicated that CYP family members and conjugation products differ between vertebrates and invertebrates [7 – 11]. For example, CYP1A family members are important phase-1 enzymes in the metabolism of aryl compounds in vertebrates, but no sequence data are available for CYP1A family members in invertebrates [9 – 12]. Moreover, glucuronides, sulfates, and glutathione-derived conjugates are typical phase-2 metabolites of aryl compounds formed in vertebrates [2]. On the other hand, the major phase-2 metabolites of aryl compounds in invertebrates are glucosides and sulfates [13–17]. Furthermore, several studies have shown that invertebrates form conjugation metabolites that have never been confirmed in vertebrates [17, 18]. Our previous study also indicated that the aquatic crustacean *Daphnia magna* forms conjugation metabolites of pyrene that have not been reported previously [7]. These results indicated that invertebrates have unique mechanisms for the metabolism of xenobiotics as compared to vertebrates. Invertebrates account for 95% of the total biomass of animals, and are therefore important components of the ecosystem. However, there is still insufficient information regarding the mechanisms of xenobiotic metabolism by invertebrates. To gain a better understanding of the impact of anthropogenic and natural toxins in the ecosystem, it is important to elucidate the mechanisms of xenobiotic metabolism and the physiological functions in invertebrates.

The present study was performed to investigate the mechanisms of xenobiotic metabolism of crustaceans, which are the predominant invertebrates in aquatic environments. We exposed freshwater decapoda; atyidae; *Caridina multidentata*, *Neocaridina denticulate*, and *Paratya compressa*, which generally inhabit Japanese rivers, to pyrene. In addition, we investigated the formation of pyrene metabolites paying special attention to phase-2 metabolites.

Structural identification of metabolites was performed by both enzymatic deconjugation and high-performance liquid chromatography (HPLC) with an electrospray ionization triple quadrupole mass spectrometry detector (ESI-MS/MS). Furthermore, we compared the mechanisms of xenobiotic metabolism in these freshwater decapoda to those in other species, and estimated the characteristics of xenobiotic metabolism of aquatic invertebrates.

# 2. Materials and methods

### *2.1. Chemicals*

Pyrene was obtained from Kanto Chemical Co., Inc. (Tokyo, Japan). 1-Hydroxypyrene, sulfatase (from limpets Type V; 34 units $mg^{-1}$), β-glucosidase (from almonds; 3.4 units $mg^{-1}$), and β-glucuronidase (from bovine liver, Type B-1; 1240 units $mg^{-1}$) were obtained from Sigma-Aldrich Co. (St. Louis, MO, USA).

### *2.2. Experimental animals*

*C. multidentata* and *N. denticulate* were captured from the river in Kitakyushu City (Southwest Japan), and *P. compressa* was obtained from the National Institute for Environmental Studies (Tsukuba, Japan). Each organism was kept in the laboratory at 20°C under a 16-h light/8-h dark photoperiod in aged tap water with commercial shrimp food.

### *2.3. Exposure of each organism to pyrene*

In this experiment, we used only adult freshwater shrimp that had been starved for 8–24 h. Ten individuals of each species were exposed to 0.67 mg $l^{-1}$ of pyrene (2 ml of 500 mg $l^{-1}$ pyrene in ethanol added to 1.5 L of

water). As a control, pyrene was not added (2 ml of ethanol was added). The exposure experiment was performed at 20°C in the dark for 24 h.

*2.4. Analysis of pyrene metabolites*

Cleanup and analytical methods of pyrene metabolites were based on the methods described in our previous study [7]. Briefly, after 24-h exposure, water was filtered with a glass filter (GF/C; Whatman, Int. Ltd., Kent, UK). The filtered water was then passed through a solid-phase cartridge (PS-2 plus; Waters, Milford, MA, USA), and eluted with 10 ml of 70% methanol. The methanol solution was dried under a gentle stream of nitrogen gas, and re-solved in 0.5 ml of methanol. Pyrene metabolites were determined by HPLC (LC-VP series; Shimadzu, Kyoto, Japan) with a fluorescence detector (FD) (RF-10AXL; Shimadzu) equipped with an ODS column (Inertsil ODS-3 150 mm×2.1 mm I.D. (5 μm); GL Sciences, Inc.). The HPLC conditions were as follows. Aliquots of 5 μl of each sample were injected and separated using a linear gradient of aqueous buffer and acetonitrile at a flow rate of 0.2 ml $min^{-1}$. The buffer consisted of 10 mM ammonium acetate, adjusted to pH 5 with 10 mM acetic acid. The gradient was programmed as follows: $t$=0 min: 20% acetonitrile, $t$=27 min: 40% acetonitrile, $t$=42 min: 100% acetonitrile, isocratic at 100% acetonitrile for 5 min. The column temperature was kept at 45°C. Excitation (EX) and emission (EM) wavelengths for FD were 343 nm and 385 nm, respectively.

*2.5. LC/ESI-MS/MS system*

HPLC (NANOSPACE SI-2 series; Shiseido Co., Ltd., Tokyo, Japan) with an electrospray ionization triple quadrupole mass spectrometry detector (ESI-MS/MS) (API 3000$^{TM}$ LC/MS/MS system; Applied Biosystems, CA, USA) was used to identify the pyrene metabolites formed by each organism. The chromatographic method used was identical to those described above . The ESI conditions were full scan (*m/z* 50 to *m/z* 700) negative mode with ion source voltage of –4.2 kV and an ion source temperature of 420°C.

*2.7. Deconjugation*

Deconjugation was performed based on the method described by Kukkonen and Oikari [14]. Briefly, sulfatase, β-glucuronidase, and β-glucosidase were dissolved in 0.1 M sodium acetate buffer (pH 5.0) to concentrations of 20 units $ml^{-1}$, 6000 units $ml^{-1}$, and 28 units $ml^{-1}$, respectively. The methanol solution was concentrated under a gentle stream of nitrogen gas, dissolved in 300 μl of 0.1 M sodium acetate buffer (pH 5.0), and 700 μl of each deconjugation enzyme was added. In the controls, 1 mg of bovine serum albumin was added. After 8 h of incubation at 37°C, 1000 μl of methanol was added to stop the reaction. The deconjugated compounds were analyzed by both LC/FD and LC/ESI-MS/MS.

## 3. Results and Discussion

*3.1. Characterization of pyrene metabolites formed by each organism*

Fig. 1 shows LC/FD chromatograms seen with pyrene exposure (A: control, B: *C. multidentata*, C: *N. denticulate*, and D: *P. compressa*). Seven characteristic peaks (peak-a, peak-b, peak-c, peak-d, peak-e, peak-f, and peak-g) were observed in the pyrene exposure treatment group, but not in the controls. Thus, these seven peaks were considered to be pyrene-derived substances. The retention times (Rt) of each peak are shown in Table 1. The major peaks observed in *C. multidentata*, *N. denticulate*, and *P. compressa* were peak-f, peak-g, and peak-e, respectively.

Fig. 2 shows the full scan ESI negative mass spectra of peak-e (Rt of 23.5 min), peak-f (Rt of 29.3 min), and peak-g (Rt of 30.2 min). The precursor ions of peak-a, peak-b, peak-c, and peak-d could not be identified, because of their low concentration or ionization disturbance by other impurities. However, in precursor ion scan mode of *m/z* 217 (characteristic *m/z* of 1-hydroxypyrene), several ions were obtained from these peaks (data not shown). Thus, peak-a, peak-b, peak-c, and peak-d were considered to be the conjugation products of 1-hydroxypyrene. On the other hand, peak-e contained major ions at *m/z* 439, 415, 379, and 217. Stroomberg *et al.* [18] demonstrated that 1-hydroxypyrene glucoside (MW = 380) was found at *m/z* of 439 ($ESI^-$). This ratio 60 *m/z* units higher than the expected *m/z* of deprotonated 1-hydroxypyrene glucoside (*m/z* = 379) is indicative of acetate adduct formation during ionization. Thus, peak-e (*m/z* = 439) was considered to be the 1-hydroxypyrene glucoside. Peak-g (RT = 30.2 min) contained a major ion at *m/z* 297. Our previous

study showed that Rt of 1-hydroxypyrene sulfate was 30.2 min, consistent with the Rt of peak-g [7]. The *m/z* 297 also corresponds to the molecular ion of deprotonated 1-hydroxypyrene sulfate. Thus, peak-g (Rt = 30.2 min) was considered to be 1-hydroxypyrene sulfate. On the other hand, peak-f (Rt = 29.3 min) contained a major ion at *m/z* 459. Our previous study showed that *D. magna* also forms a pyrene metabolite with the major ion of *m/z* 459, although its Rt did not correspond to peak-f (Rt of *m/z* 459 metabolites formed by *D. magna* was 23.3 min) [7]. To our knowledge, the structure of the pyrene metabolite at *m/z* 459 has not been reported previously, and is therefore considered to be a new pyrene metabolite.

*3.4. Structure of the new phase-2 metabolite (peak-f) formed by freshwater shrimp; decapoda; atyidae*

To identify the structure of the new pyrene metabolite (peak-f) formed by *C. multidentata, N. denticulate*, and *P. compressa*, the metabolite was treated with sulfatase, β-glucuronidase, and β-glucosidase (Fig. 3). The Rt and mass spectrum of peak-f showed no changes with β-glucuronidase or β-glucosidase treatment. However, with sulfatase treatment, Rt of peak-f shifted to 23.5 min, and the mass spectrum changed to *m/z* 439, 415, and 217 (Fig. 3B; peak-f2). The Rt and mass spectrum of peak-f2 were consistent with peak-e, which is considered to be the 1-hydroxypyrene glucoside. Peak-f2 was further treated with sulfatase, β-glucuronidase, and β-glucosidase. The Rt and mass spectrum did not change after sulfatase or β-glucuronidase treatment. On the other hand, with β-glucosidase treatment, the Rt of peak-f2 shifted to 37.1 min and the mass spectrum changed to *m/z* 217 (Fig. 3C; peak-f3). The Rt and mass spectrum of peak-f3 were consistent with 1-hydroxypyrene. Our results of deconjugation indicated that glucose and sulfate combined with 1-hydroxypyrene. In addition, the molecular order of the combination was sulfate, glucose, and 1-hydroxypyrene.

Fig. 4 shows the LC/ESI-MS/MS mass spectra of the product ion of *m/z* 459. We showed that the major fragment was *m/z* 241 with minor fragments of *m/z* 379, 289, 259, and 97. The major fragment with *m/z* 241 could be attributed to the glucoside-sulfate moiety after the neutral loss of 1-hydroxypyrene. The fragment of *m/z* 379 formed after loss of the sulfate moiety (neutral loss = 80). The fragment with *m/z* 97 was considered to be the sulfate moiety. On the other hand, those at *m/z* 259 and *m/z* 289 were considered to be the common fragments of glycoconjugates [18, 19]. Our results of LC/ESI-MS/MS analysis and deconjugation indicated that peak-f was the glucose-sulfate conjugate of 1-hydroxypyrene. Glucose-sulfate conjugate was a conjugation product that has not been reported previously in any organism. On the other hand, the LC/ESI-MS/MS fragment pattern of the *m/z* 459 metabolite formed by *D. magna* was rather different from that of the glucose-sulfate conjugate formed by these shrimp. Thus, the *m/z* 459 metabolite formed by *D. magna* may be the isomer or a different conjugation product of 1-hydroxypyrene with the same *m/z*.

*3.5. The role of glucose-sulfate conjugation formed by freshwater shrimp; decapoda; atyidae*

Glucuronides, glucosides, sulfates, and glutathione-derived conjugates have been reported as major conjugation products of PAHs formed by various organisms [2]. On the other hand, Stroomberg *et al.* [18] determined the structure of a conjugation metabolite of pyrene formed by isopods (*Porcellio scaber*) and collembolans (*Folsomia candida*) as pyrene-1-*O*-(6”-*O*-malonyl)-glucoside, which is the first reported conjugate formed by animals. On the other hand, malonyl-glycosides are well-known conjugation products formed by plants [19–24]. Glucose conjugates formed by various plants are often further conjugated by malonic acid or pentosyl units of hemicellulose, such as apiose or xylose, and form glucose-malonate or glucose-pentosyls [19–24]. Day and Saunders [23] demonstrated roles of these additional conjugation processes as signals of sequestration of phase-2 metabolites in the plant cell (phase-3 processes for plants). For example, apiose-glycosides of chlorophenols formed by *Lemna minor* are sequestrated into cell walls, and malonyl-glycosides are sequestrated into vacuoles [23]. These observations indicated that glucose conjugates further conjugated with malonic acid or apiose could have a specific signal for sequestration in plant cells.

We showed that freshwater shrimp (decapoda; atyidae; *C. multidentata, N. denticulate* and *P. compressa*) metabolize pyrene to glucose-sulfate conjugates. These are the first conjugation products reported to date in any species. The glucose-sulfate conjugate of 1-hydroxypyrene is the predominant metabolite of these shrimp, especially *C. multidentata*, and therefore this metabolic process is considered important. However, the question remains why they make glucose-sulfate conjugates although they make both glucose and sulfate

conjugates. To answer this question, we considered the role of sulfation of glucose. Sulfation of sugar commonly creates additional structural variety [25, 26]. The addition of sulfonate groups creates a negatively charged molecular environment at physiological pH that can induce conformational changes, alter solubility, and promote ionic interactions, all of which can significantly influence biological activity [25, 26]. Furthermore, ABC transporters such as Multixenobiotic Resistance Protein (MRP) and P-glycoprotein are important transporters for excretion of xenobiotics across the cell membrane (Phase-3 processes for animals) [4 – 6]. Especially, MRP is an organic anion transporter with high activity toward compounds conjugated to glutathione (GSH), glucuronide, or sulfate [27–29]. The sulfation of glucose conjugate could add a negative charge to the molecules, and may stimulate the excretion of xenobiotics by transporters such as MRP.
The aquatic environment is the major storehouse of sulfate and contains more than 95% of the total amount of sulfate on the Earth [30]. In mammals, sulfation of aryl compounds occurs predominant in the initial stage of metabolism, but is soon saturated because of exhaustion of sulfate ions, and glucuronidation then takes place [2]. However, aquatic invertebrates live under sulfate-rich conditions, and therefore they may not be subject to exhaustion of sulfate ions from their bodies. Several studies have demonstrated that sulfation is an important pathway for metabolism of xenobiotics in aquatic invertebrates [7, 13–16]. For these reasons, sulfation of glucose conjugates may add an important signal for excretion or sequestration of xenobiotics for aquatic invertebrates.

## Conclusions

In conclusion, the freshwater shrimp decapoda; atyidae; *C. multidentata, N. denticulate* and *P. compressa* metabolize pyrene to glucose-sulfate conjugates that have not been reported in other organisms. Sulfation of glucose conjugates may add an important signal for excretion or sequestration of xenobiotics from these organisms. On the other hand, metabolic responses of xenobiotics show a large degree of variation in invertebrates as compared to vertebrates. This may be due to the differences in evolution and adaptation processes in various environments between invertebrates. Knowledge regarding the metabolic mechanisms in each species could help in elucidating their evolution and adaptation processes, and thus their tolerance to environmental toxins. To gain further understanding of the toxic effects of xenobiotics on aquatic invertebrates, further studies are needed to elucidate these mechanisms.

## 4. Acknowledgments

We thank Yoshio Sugaya and Yutaka Ogamino (National Institute for Environmental Studies, Tsukuba Japan) for providing *P. compressa* samples.
We thank Dr. Takayuki Hanazato, Dr. Mayumi Ishizuka, Dr. Shoichi Fujita, Dr. Takamaru Nagata, Mr. Jing-yon Ha, Mr. Kentaro Q Sakamoto, Mr. Masaki Sakamoto, Mr. Noriaki Sakai, and Mr. Ryouhei Inuzuka for helpful suggestions regarding the experiments

## 5. References

[1] N. R. Verrengia Guerrero, M. G. Taylor, N. A. Davies, M. A. M. Lawrence, P. A. Edwards, K. Simkiss, E. A. Wider, Evidence of differences in the biotransformation of organic contaminants in three species of freshwater invertebrates, Environ. Pollut. 117 (2002) 523-530.
[2] M. J. Zamek-Gliszczynski, K. A. Hoffmaster, K. Nezasa, M. N. Tallman, K. L. R. Brouwer, Integration of hepatic drug transporters and phase Ⅱ metabolizing enzymes: Mechanisms of hepatic excretion of sulfate, glucuronide, and glutathione metabolites, Eur. J. Pharm. Sci. 27 (2006) 447-486.
[3] K. F. Rewitz, B. Styrishave, A. Løbner-Olesen, O. Andersen, Marine invertebrate cytochrome P450: Emerging insights from vertebrate and insect analogies, Comp. Biochem. Physiol. C 143 (2006) 363-381.
[4] D. Keppler, I. Leier, G. Jedlitschky, J. Köning, ATP-dependent transport of glutathione *S*-conjugates by the multidrug resistance protein MRP1 and its apical isoform MRP2, Chem-Biol. Interact. 111-112 (1998) 153-161.
[5] S. P. C. Cole, R. G. Deeley, Multidrug resistance mediated by the ATP-binding cassette transporter protein MRP, BioEssays 20 (1998) 931-940.
[6] S. M. Bard, Multixenobiotic resistance as a cellular defense mechanism in aquatic organisms, Aquat. Toxicol. 48 (2000) 357-389.

[7] Y. Ikenaka, H. Eun, M. Ishizaka, Y. Miyabara, Metabolism of pyrene by aquatic crustacean, *Daphnia magna*, Aquat. Toxicol. 80 (2006) 158-165.
[8] M. O. James, Cytochrome P450 monooxygenases in crustaceans, Xenobiotica 19 (1989) 1063-1076.
[9] M. O. James, S. M. Boyle, Cytochromes P450 crustacea, Comp. Biochem. Physiol. C 121 (1998) 157-172.
[10] K. F. Rewitz, B. Styrishave, A. Lødner-Olesen, O. Andersen, Marine invertebrate cytochrome P450: Emerging insights from vertebrate and insect analogies, Comp. Biochem. Physiol. C 143 (2006) 363-381.
[11] S. Chaty, F. Rodius, P. Vasseur, A comparative study of the expression of *CYP1A* and *CYP4* genes in aquatic invertebrate (freshwater mussel, *Unio tumidus*) and vertebrate (rainbow trout, *Oncorhynchus mykiss*), Aquat. Toxicol. 69 (2004) 81-93.
[12] R. F. Lee, J. W. Anderson, Significance of cytochrome P450 system responses and levels of bile fluorescent aromatic compounds in marine wildlife following oil spills, Mar. Pollut. Bull. 50 (2005) 705-723.
[13] R. Hryk, J. Beyer, K. Urich, Metabolism od phenol in the terrestrial snail *Cepaea nemoralis* L., Xenobiotica 22 (1992) 77-81.
[14] J. Kukkonen, A. Oikari, Sulphate conjugation is the main route of pentachlorophenol metabolism in *Daphnia magna*, Comp. Biochem. Physiol. C 91 (1988) 465-468.
[15] C. D. Simpson, W. R. Cullen, T. Y. T. He, M. Ikonomou, K. J. Reimer, Metabolism of pyrene by two clam species, *Mya arenaria* and *Protothaca staminea*, Chemosphere 49 (2002) 315-322.
[16] S. L. Shofer, R. S. Tjeerdema, Comparative disposition and biotransformation of pentachlorophenol in the oyster (*Crassostrea gigas*) and Abalone (*Haliotis fulgens*), Pestic. Biochem. Phys. 46 (1993) 85-95.
[17] G. J. Stroomberg, J. A. de Knecht, F. Ariese, C. A. M. van Gestel, N. H. Velthorst, Pyrene metabolites in the hepatopancreas and gut of the isopod *Porcellio scaber*, a new biomarker for polycyclic aromatic hydrocarbon exposure in terrestrial ecosystems, Environ. Toxicol. Chem. 18 (1999) 2217-2224.
[18] G. J. Stroomberg, H. Zappey, R. J. C. A. Steen, C. A. M. ven Gestel, F. Ariese, N. H. Velthorst, N. M. van Straalen, PAH biotransformation in terrestrial invertebrates – a new phase Ⅱ metabolite in isopods and springtails, Comp. Biochem. Physiol. C 138 (2004) 129-137.
[19] W. Bylka, R. Franski, M. Stobiecki, Differentiation between isomeric acacetin-6-*C*-(6”-*O*-malonyl) glucoside and acacetin-8-*C*-(6”-*O*-malonyl) glucoside by using low-energy CID mass spectra, J. Mass. Spectrom. 37 (2002) 648-650.
[20] P. Bednarek, R. Frański, L. Kerhoas, J. Einhorn, P. Wojtaszek, M. Stobiecki, Profiling changes in metabolism of isoflavonoids and their conjugates in *Lupinus albus* treated with biotic elicitor, Phytochemistry 56 (2001) 77-85.
[21] I. Cummins, M. Brazier-Hicks, M. Stobiecki, R. Frański, R. Edwards, Selective disruption of wheat secondary metabolism by herbicide safeners, Phytochemistry 67 (2006) 1722-1730.
[22] T. Ishii, M. Yanagisawa, Synthesis, separation and NMR spectral analysis of methyl apiofuranosides, Carbohyd. Res. 313 (1998) 189-192.
[23] J. A. Day, F. M. Saunders, Glycosidation of chlorophenols by *Lemna minor*, Environ. Toxicol. Chem. 23 (2004) 613-620.
[24] R. Schmitt, J. Kaul, T. V. D. Trenck, E. Schaller, H. Sandermann, Jr., β-D-Glucosyl and *O*-malonyl-β-D-glucosyl conjugates of pentachlorophenol in soybean and wheat: Identification and enzymatic synthesis, Pestic. Biochem. Phys. 24 (1985) 77-85.
[25] C. A. Strott, Sulfonation and Molecular Action, Endocr. Rev. 23 (2002) 703-732.
[26] L. V. Hooper, S. M. Manzella, J. U. Baenziger, From legumes to leukocytes: Biological roles for sulfated carbohydrates, FASEB J. 10 (1996) 1137-1146.
[27] J. Cummings, N. Zelcer, J. D. Allen, D. Yao, G. Boyd, M. Maliepaard, T. H. Friedberg, J. F. Smyth, D. I. Jodrell, Biochem. Pharmacol. 67 (2004) 31-39.
[28] M. Kool, M. van der Linden, M. de Haas, G. L. Scheffer, J. M. L. de Vree, A. J. Smith, G. Jansen, G. J. Peters, N. Ponne, R. J. Scheper, R. P. J. O. Elferink, F. Baas, P. Borst, Proc. Natl. Acad. Sci. USA 96 (1999) 6914-6919.
[29] A. Geier, M. Wagner, C. G. Dietrich, M. Trauner, Principles of hepatic organic anion transporter regulation during cholestasis, inflammation and liver regeneration, BBA 1773 (2007) 283-308

[30] H. J. M. Bowen, Environmental chemistry of the elements, Academic press, London, 1979.

## Figure captions

Figure 1: LC/FD chromatogram of pyrene metabolites formed by freshwater decapoda atyidae. A. Chromatogram of control. B, C, and D. Chromatograms of *C. multidentata*, *N. denticulate*, and *P. compressa*, respectively. Seven characteristic peaks (peak-a, peak-b, peak-c, peak-d, peak-e, peak-f, and peak-g) were observed in pyrene exposure treatment groups, but not in the controls. Excitation (EX) and emission (EM) wavelengths for FD were 343 nm and 385 nm, respectively. The gradient program of HPLC (acetonitrile concentration) is also shown in A (right axis).

Figure 2: Electrospray ionization MS spectra of peak-e, peak-f, and peak-g. Peak-e, peak-f, and peak-g showed dominant masses of *m/z* 439, *m/z* 459, and *m/z* 297, respectively.

Figure 3: Electrospray ionization MS spectra of: (A) peak-f; (B) after sulfatase treatment of peak-f (peak-f2); and (C) after β-glucosidase treatment of peak-f2 (peak-f3). Peak-f2 and peak-f3 showed dominant masses of *m/z* 439 and *m/z* 217, respectively.

Figure 4: Electrospray ionization MS and $MS^2$ spectra of peak-f. The ESI conditions were full scan (*m/z* 50 to *m/z* 700) negative mode. The metabolite of peak-f contained a major ion at *m/z* 459 (MS) with product ions of *m/z* 379, 289, 259, 241, and 97 ($MS^2$).

**Table 1: Characteristics of pyrene metabolites**

| Pyrene metabolits | RT (min) | MS (*m/z*) | $MS^2$(*m/z*) |
|---|---|---|---|
| Peak-a | 5.3 | - | - |
| Peak-b | 6.8 | - | - |
| Peak-c | 7.8 | - | - |
| Peak-d | 16.5 | - | - |
| Peak-e | 23.5 | 439, 415, 375 217 | 217 |
| Peak-f | 29.3 | 459 | 459, 379, 289, 259, 241, 97 |
| Peak-g | 30.2 | 297, 217 | 217 |
| | | | |
| 1-Hydroxypyrene glucuronide | 17.5 | 393, 217 | 217 |
| 1-Hydroxypyrene sulfate | 30.2 | 297, 217 | 217 |
| 1-Hydroxypyrene | 37.1 | 217 | - |
| Pyrene | 42.0 | - | - |

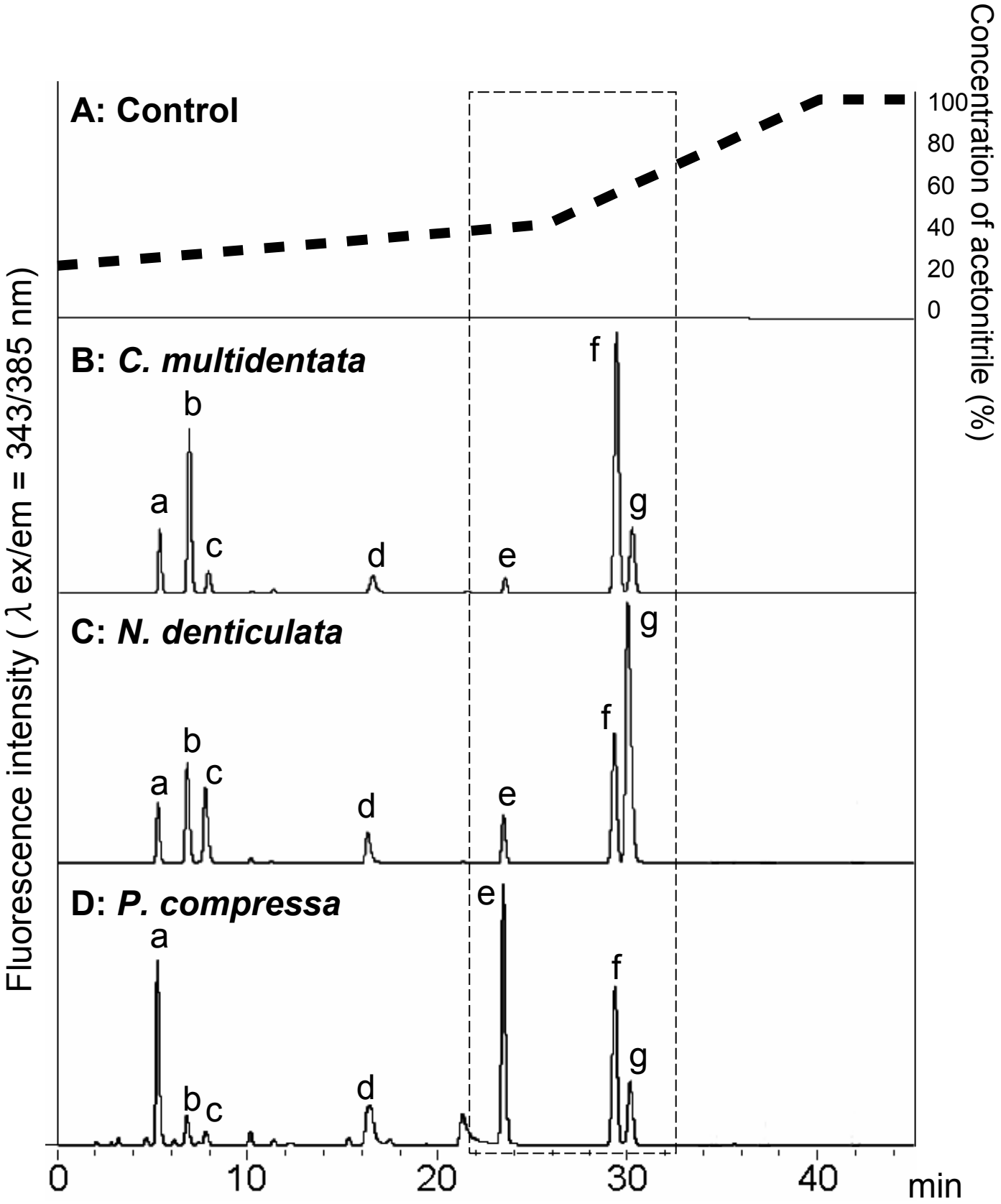
A: Control
B: C. multidentata
C: N. denticulata
D: P. compressa
a
b
c
d
e
f
g
Fluorescence intensity ( λ ex/em = 343/385 nm)
Concentration of acetonitrile (%)
100
80
60
40
20
0
0
10
20
30
40
min

Figure 2

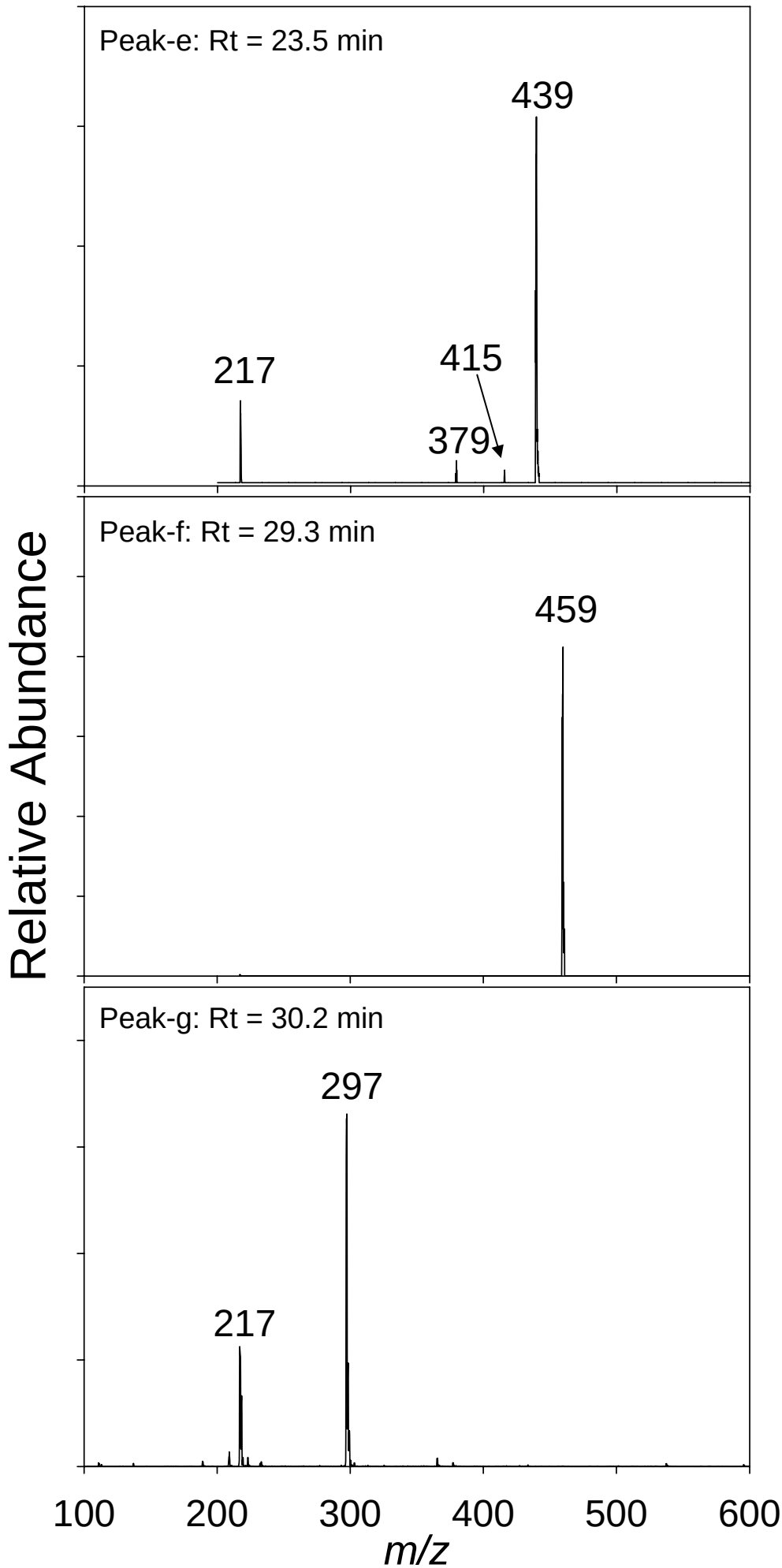
Peak-e: Rt = 23.5 min
439
217
415
379
Peak-f: Rt = 29.3 min
459
Peak-g: Rt = 30.2 min
297
217
Relative Abundance
100
200
300
400
500
600
m/z

Figure 3

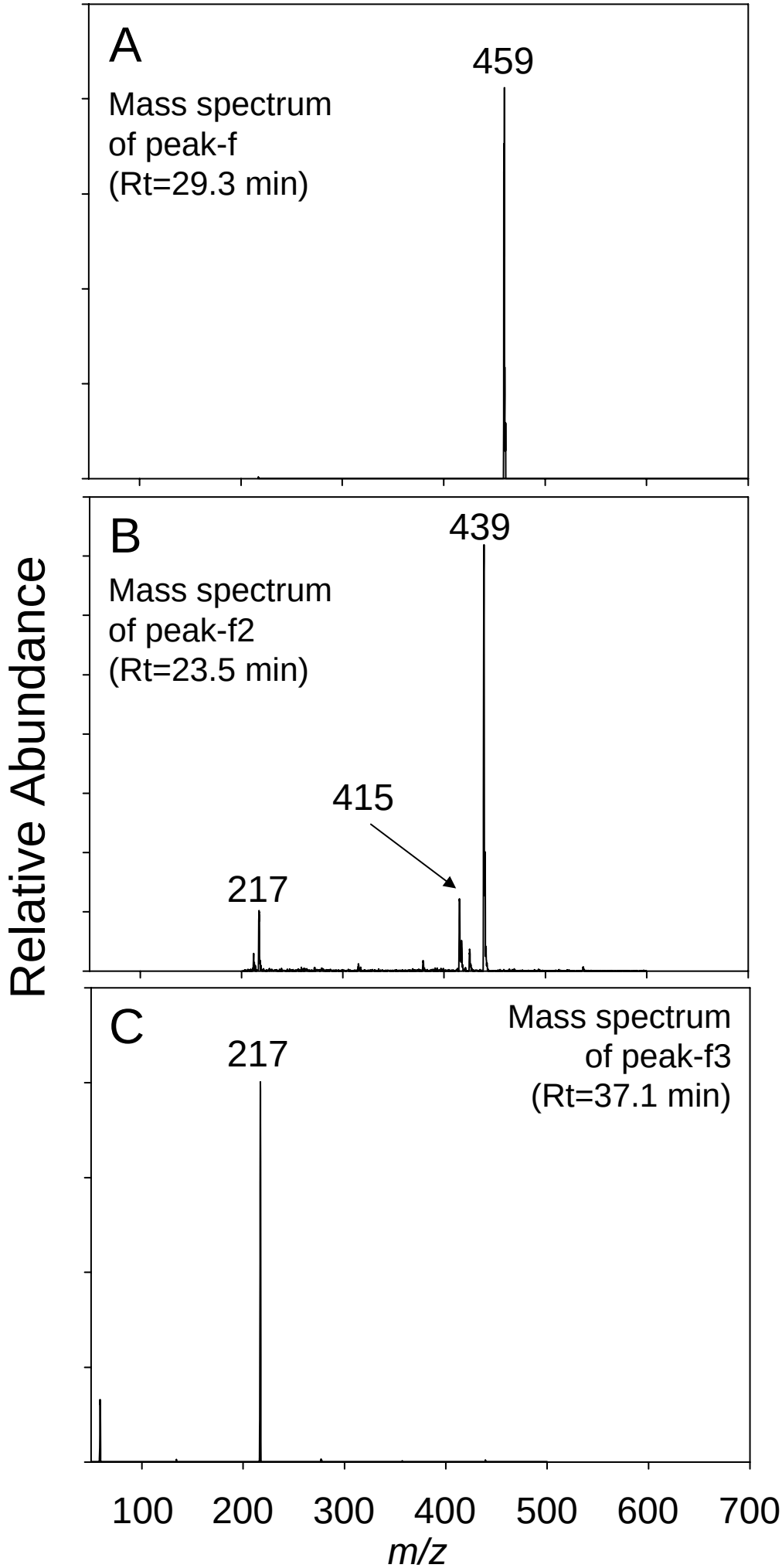
A
459
Mass spectrum
of peak-f
(Rt=29.3 min)
B
439
Mass spectrum
of peak-f2
(Rt=23.5 min)
415
217
C
217
Mass spectrum
of peak-f3
(Rt=37.1 min)
Relative Abundance
100
200
300
400
500
600
700
m/z

Figure 4

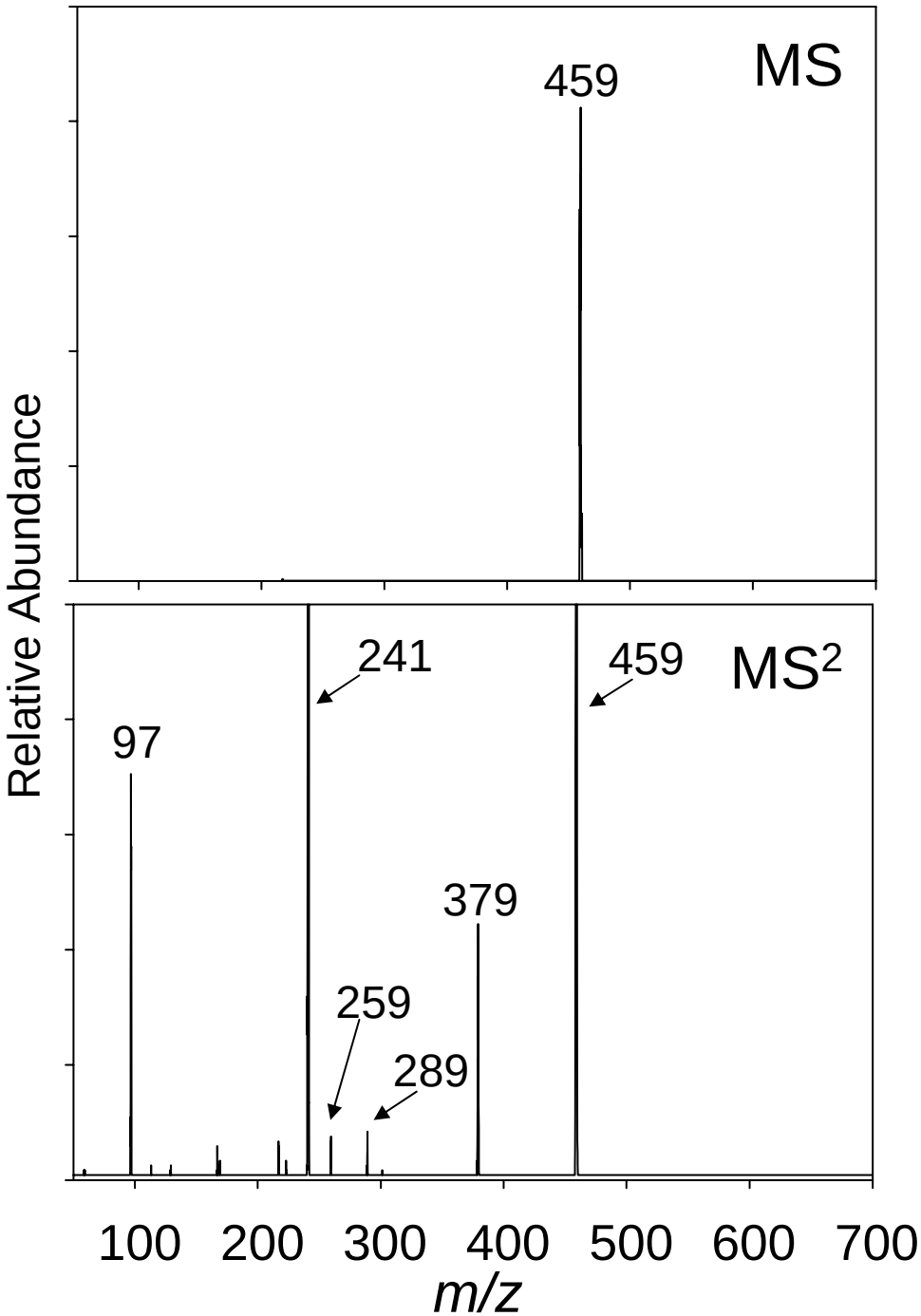


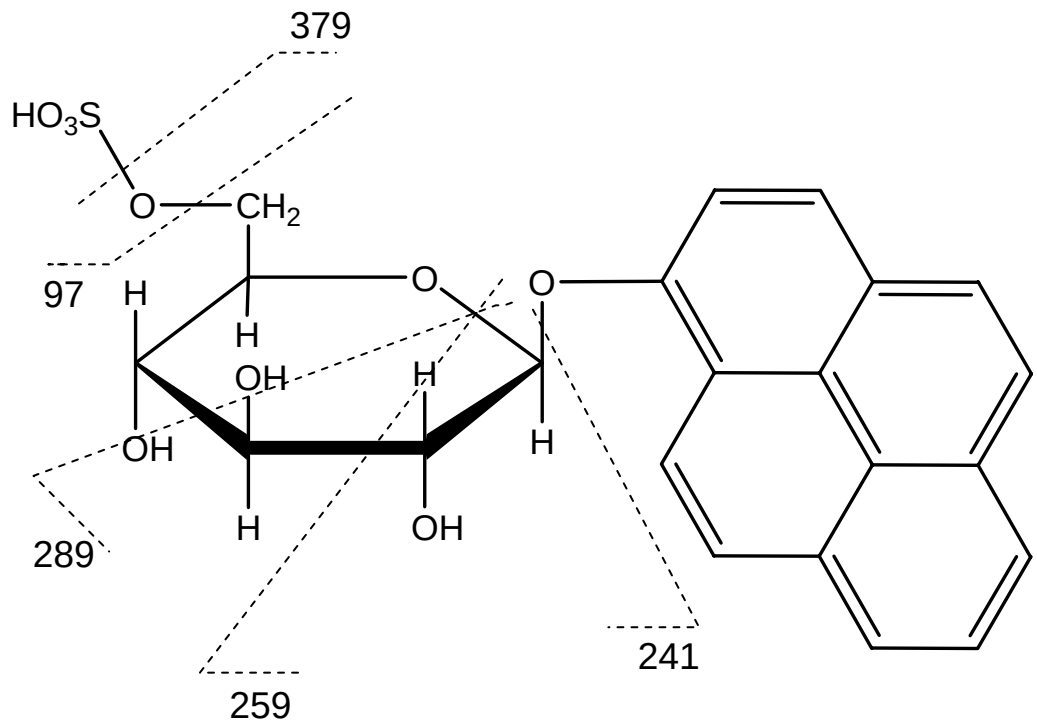


MW = 460: glucose sulfate conjugate of 1-hydroxypyrene